

JIN KYEONG SHIN¹, SU MIN EUN¹, YEONG TAE CHOI², BYUNG JOON CHOI^{1*}

UV PULSE SEQUENCE-DEPENDENT PROPERTIES OF Al₂O₃ FILMS VIA UV-ASSISTED ATOMIC LAYER DEPOSITION

Uniform thin-film deposition on temperature-sensitive or particulate substrates remains challenging at low temperatures. Energy-enhanced atomic layer deposition offers an effective approach to activate surface reactions by supplying external energy such as plasma, mechanical input, or photon irradiation. In this work, Al₂O₃ thin films were deposited at a low temperature of 85°C by UV-assisted atomic layer deposition, and the effects of UV irradiation conditions on film properties were investigated. Under UV irradiation, the growth rate increased, while surface roughness and residual carbon content decreased, accompanied by an increase in the Al–O bonding fraction. These results demonstrate that UV-assisted atomic layer deposition enables high-quality Al₂O₃ coatings even under low-temperature conditions and suggest its potential applicability to powder surface modification processes.

Keywords: UV-assisted atomic layer deposition; low temperature process; Al₂O₃ thin film; surface reaction

1. Introduction

Atomic layer deposition (ALD) has been widely employed for uniform thin-film growth on a variety of substrates, such as high-aspect-ratio structures with irregular shapes [1-3]. However, conventional thermal ALD requires elevated process temperatures (>200°C), limiting its applicability to thermally sensitive substrates, such as polymers, reactive particles, and biomaterials [4-7].

To enable low-temperature ALD, energy-enhanced ALD techniques have been introduced [8-10]. Plasma is one of the most widely used energy sources in energy-enhanced ALD, employing various plasma generation methods such as microwave plasma, capacitively coupled plasma (CCP), and inductively coupled plasma (ICP); however, plasma-induced damage and non-uniform radical density remain critical concerns, particularly for sensitive substrates. Alternatively, UV-assisted atomic layer deposition (UV-ALD) was adopted in this study. In UV-ALD, photon energy promotes ligand photodecomposition and surface reactions, enabling efficient film growth at reduced temperatures [11,12]. Previous studies have demonstrated oxide thin-film deposition using UV-ALD. Yoon et al. reported low-temperature UV-ALD of Al₂O₃ thin films for gas-diffusion barrier applica-

tions and demonstrated the beneficial effect of UV irradiation [11]. However, their study mainly focused on the overall UV effect and did not provide a sufficiently detailed mechanistic discussion of how UV irradiation affected the surface reactions. In addition, they did not investigate how film properties changed with increasing UV exposure time. In contrast, Kim et al. investigated UV-ALD of TiO₂ thin films by varying the irradiation timing while keeping the UV exposure duration constant, applying UV either after the metal precursor pulse or after the oxidant pulse [12]. Since TiO₂ and Al₂O₃ differ in precursor chemistry, surface reaction pathways, and ligand removal behavior, the UV-assisted reaction mechanism cannot be assumed to be identical for the two material systems. Therefore, a systematic study that directly compares both UV irradiation timing and UV exposure duration within the Al₂O₃ system is still lacking.

In this work, Al₂O₃ thin films were deposited on Si substrates, and the effects of UV irradiation were quantitatively evaluated through a direct comparison of thermal ALD and UV-ALD processes. Specifically, both the UV irradiation timing and exposure duration were systematically optimized to enable low-temperature deposition and to clarify how UV pulse design influences the growth behavior and film properties of Al₂O₃ thin films.

¹ SEOUL NATIONAL UNIVERSITY OF SCIENCE AND TECHNOLOGY, DEPARTMENT OF MATERIAL SCIENCE AND ENGINEERING, SEOUL 01811, KOREA

² MAJE TECHNOLOGY CO. LTD., SUWON 16426, GYEONGGI, KOREA

* Corresponding author: bjchoi@seoultech.ac.kr



2. Experimental

In this study, Al₂O₃ thin films were deposited on bare Si substrates using trimethylaluminum (TMA) and H₂O as the Al precursor and oxidant, respectively, as shown in Fig. 1(a). A commercial UV-ALD (MAJE Technology, Korea) was built for this work. UV irradiation was applied through a quartz window using a UV-C lamp (200-280 nm, 40 W), and all films were deposited for 100 ALD cycles at 85°C. For UV-ALD, a UV irradiation step was incorporated into the conventional thermal ALD cycle with varied irradiation timing, as shown in Fig. 1(b). The thermal ALD cycle consisted of TMA dosing – N₂ purging – H₂O dosing – N₂ purging. According to the UV irradiation timing, the samples were designated as TMA-UV, H₂O-UV, UV-1s, UV-2s, UV-5s, and UV-10s. The TMA-UV sample was obtained by applying UV irradiation immediately after TMA dosing, as shown in step (1), followed by an additional purge step to remove residual by-products. The H₂O-UV sample was obtained by applying UV irradiation immediately after H₂O dosing, as shown in step (2), followed by a purge step. For the UV-1s, UV-2s, UV-5s, and UV-10s samples, UV irradiation was initiated simultaneously with the 0.5 s H₂O dosing step, as shown in step (3), and further maintained during the subsequent H₂O purge step for an additional 0.5, 1.5, 4.5, and 9.5 s, respectively, corresponding to total UV exposure times of 1, 2, 5, and 10 s. Film surface roughness, thickness, morphology, and chemical bonding states were characterized by atomic force microscopy (AFM, NX10, Park Systems), ellipsometry (FS-1, Film Sense), high-resolution field emission scanning electron microscopy (HR-SEM, SU8010, Hitachi High Technologies Corporation), and X-ray photoelectron spectroscopy (XPS, Nexsa, Thermo Fisher Scientific), respectively.

3. Results and discussion

Cross-sectional HR-SEM images in Fig. 2(a)-(f) confirmed that all films were uniformly deposited across the entire substrate. Thickness measurements obtained using ellipsometry and HR-SEM subsequently showed that the UV-ALD films were consistently thicker than the thermal ALD film, indicating an enhanced growth-per-cycle (GPC) under UV irradiation. Specifi-

cally, the GPC increased from 1.61 Å/cycle for thermal ALD to 1.84 (TMA-UV), 1.79 (H₂O-UV), 1.81 (UV-1s), 1.76 (UV-2s), 1.71 (UV-5s), and 1.79 Å/cycle (UV-10s), thereby demonstrating higher GPC for all UV-irradiated conditions than for the thermal process.

The AFM surface morphologies of selected films are presented in Fig. 2(g)-(i). The Thermal ($R_q = 0.232$ nm), H₂O-UV ($R_q = 0.231$ nm), and short UV exposure (UV-1s, $R_q = 0.248$ nm) samples exhibited comparable surface roughness despite an increased GPC under UV irradiation. In contrast, the TMA-UV exhibited the highest roughness ($R_q = 0.977$ nm), which may be related to non-uniform photochemical removal of surface Al-CH₃ species and localized surface activation, resulting in less uniform film growth [13]. With sufficient UV irradiation (UV-10s), the surface roughness was significantly reduced to $R_q = 0.189$ nm, indicating more uniform surface reactions and smoother Al₂O₃ film formation.

The XPS spectra of Al 2p and O 1s are presented in Fig. 3. Peak deconvolution of Al 2p into main Al-O bonding and OH⁻ related bonding in Fig. 3(a) revealed that the Al-O bonding fraction increased from 55.7% (Thermal) to higher values in all UV-ALD samples, reaching a maximum of 70.6% for UV-10s. This increase in the Al-O binding fraction indicates enhanced ligand removal and oxygen bonding [14,15]. In the case of O 1s shown in Fig. 3(b), the Al-O bonding energy was shifted to lower binding energy in TMA-UV, while the peaks of the other samples remained unchanged. In addition, the carbon content was quantified from the XPS C 1s narrow-scan spectra after an initial survey scan and subsequent Ar ion sputtering, with sensitivity-factor correction applied. To minimize the contribution from adventitious carbon contamination on the sample surface, the reported carbon values were obtained after Ar ion sputtering. The carbon content decreased slightly from 1.16 at.% (Thermal) to 0.95 at.% (TMA-UV) and 0.93 at.% (H₂O-UV). With increasing UV irradiation time, the carbon content decreased from 1.07 at.% (UV-1s) to 0.88 at.% (UV-10s), indicating that prolonged UV exposure promoted the removal of residual organic ligands.

Fig. 4 shows the plausible reaction mechanism for thermal ALD and the UV-10s condition. In thermal ALD (Fig. 4(a)), incomplete surface reactions may leave residual ligands on the surface, whereas in the UV-10s condition (Fig. 4(b)), prolonged

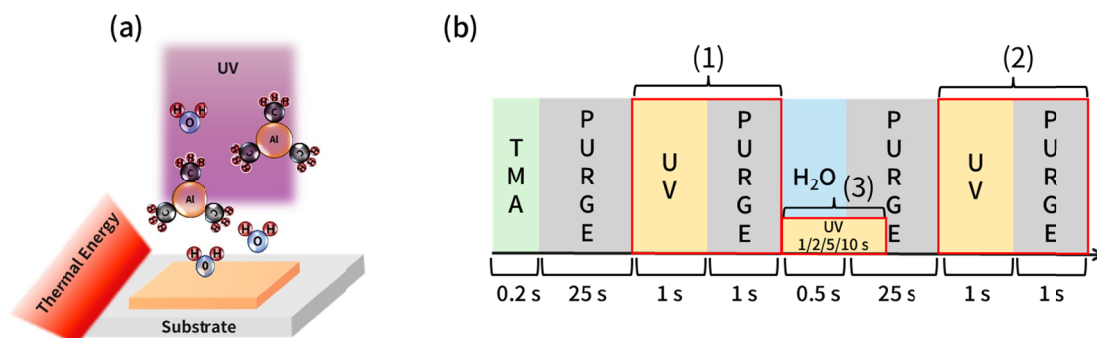


Fig. 1. (a) Schematic of UV-ALD of Al₂O₃. (b) UV-ALD process recipes with different UV irradiation conditions: (1) TMA-UV, (2) H₂O-UV, and (3) UV-1s, UV-2s, UV-5s and UV-10s

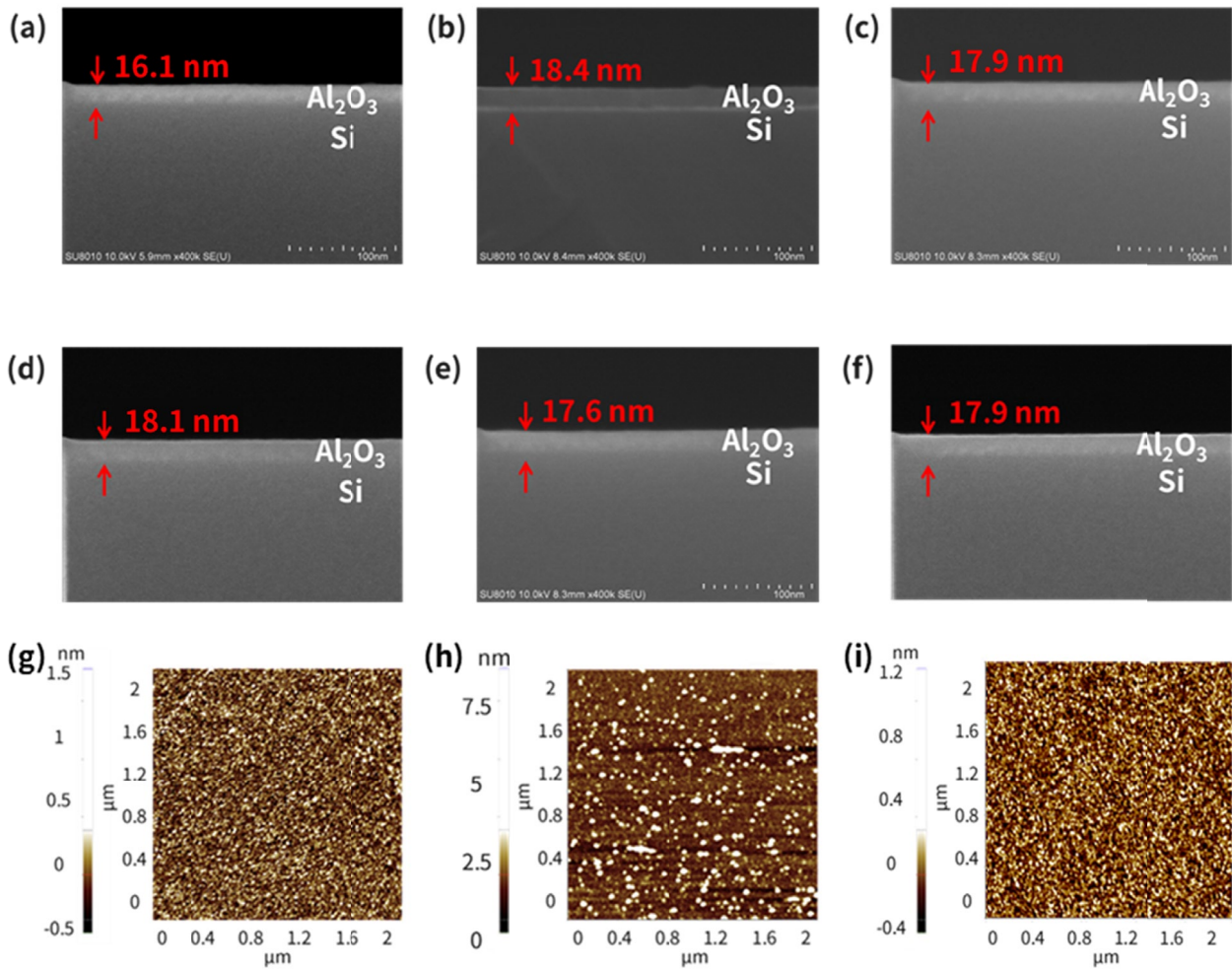


Fig. 2. (a)-(f) Cross-sectional HR-SEM images of Al_2O_3 thin films deposited under (a) Thermal, (b) TMA-UV, (c) H_2O -UV, (d) UV-1s, (e) UV-2s, and (f) UV-10s conditions. (g)-(i) AFM surface morphology images of Al_2O_3 thin films deposited under (g) Thermal, (h) TMA-UV, and (i) UV-10s conditions

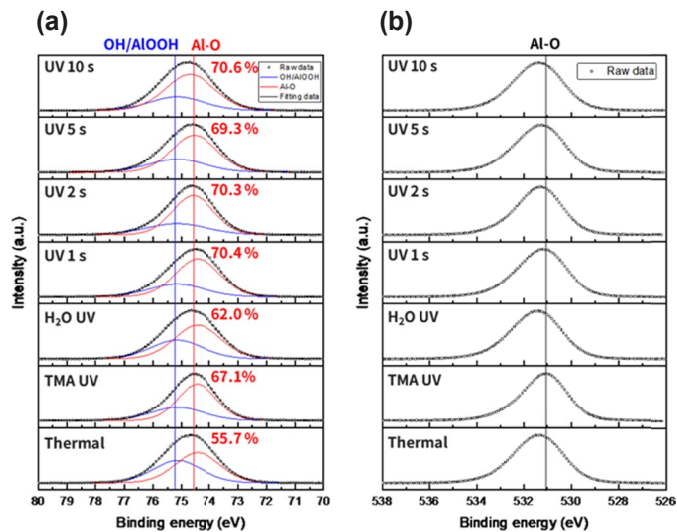


Fig. 3. XPS spectra of Al_2O_3 thin films (a) Al 2p, (b) O 1s

UV irradiation during the H_2O half-cycle may promote more effective ligand removal and modify the surface reaction pathway. In the TMA-UV condition, UV irradiation is applied immediately after the TMA pulse, when surface Al-CH_3 -containing species

are expected to remain after TMA adsorption. Under this condition, UV irradiation may promote localized photochemical removal of these ligands, which is consistent with the highest GPC observed among the investigated conditions. However, because this UV-assisted reaction may occur non-uniformly across the surface, the TMA-UV condition also exhibited the highest surface roughness. In the H_2O -UV condition, UV irradiation is applied after the H_2O pulse, when the surface is expected to be hydroxyl-terminated. Under this condition, the surface may be relatively stable compared to the TMA-UV or concurrent UV-assisted conditions, so UV irradiation may contribute more to the removal of physisorbed H_2O and residual surface by-products than to direct ligand removal. This interpretation is consistent with the relatively smooth surface of H_2O -UV, although the Al-O bonding fraction was the lowest among the investigated UV-assisted conditions. When UV irradiation was applied concurrently with H_2O dosing, the UV-1s condition showed roughness and GPC comparable to those of H_2O -UV while exhibiting a higher Al-O bonding fraction, suggesting more effective surface reactions than those in H_2O -UV. Notably, the UV-10s condition, with the longest UV exposure time, produced the smoothest surface, the highest Al-O bonding

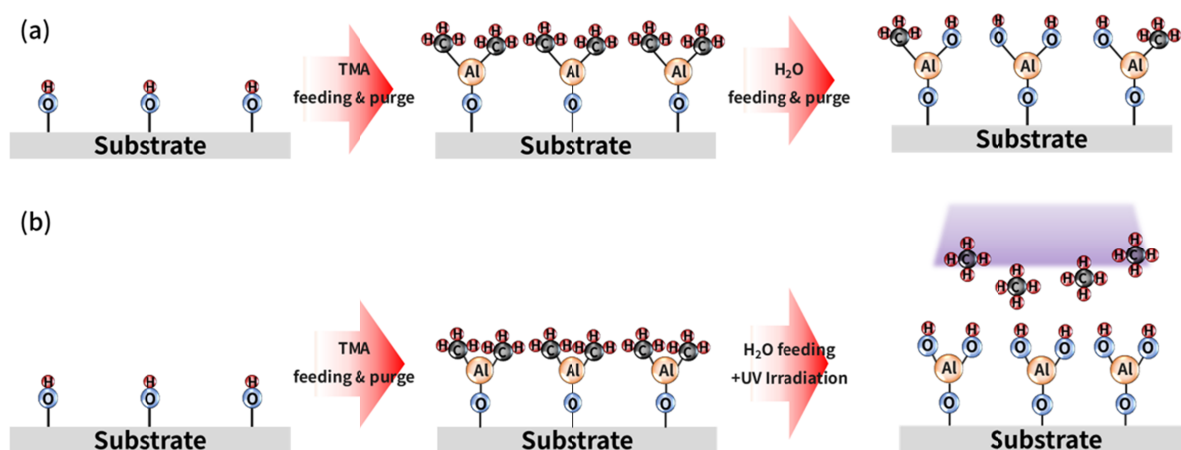


Fig. 4. Reaction mechanisms of Al_2O_3 thin films: (a) Thermal, (b) UV-10s

fraction, and the lowest carbon content, indicating the most effective ligand removal and the highest film quality among the investigated conditions.

Overall, these results suggest that the effect of UV irradiation is strongly governed by its timing and duration within the ALD cycle. In particular, prolonged UV irradiation applied concurrently with H_2O dosing appears to provide the most favorable balance among growth behavior, surface smoothness, and chemical bonding characteristics, enabling the formation of low-carbon, high-quality Al_2O_3 films even at low temperatures.

4. Conclusions

High-quality Al_2O_3 thin films were deposited at 85°C by UV-ALD, indicating that UV irradiation can partially compensate for the limited thermal budget at low temperatures. Systematic variation of the UV pulse sequence and exposure time revealed a strong dependence of both growth behavior and film quality on the irradiation scheme. UV irradiation following the TMA pulse increased the GPC but was accompanied by higher surface roughness, whereas UV irradiation following the H_2O pulse yielded smoother films but with a lower Al-O bonding fraction. Notably, a sufficiently long 10 s UV irradiation applied concurrently with H_2O dosing produced Al_2O_3 films with the smoothest surface, the highest Al-O bonding fraction, and the lowest carbon content at 85°C . These results underscore the critical role of UV pulse design in UV-ALD and highlight its potential for low-temperature, conformal Al_2O_3 coatings, including powder surface modification.

Acknowledgments

This work was supported by the National Research Foundation of Korea (NRF) grant funded by the Korea government (MSIT) (NRF-2023R1A2C1006831).

REFERENCES

- [1] S.M. George, *Chem. Rev.* **110**, 111-131 (2010). DOI: <https://doi.org/10.1021/cr900056b>
- [2] R.W. Johnson, A. Hultqvist, S.F. Bent, *Mater. Today* **17**, 236-246 (2014). DOI: <https://doi.org/10.1016/j.mattod.2014.04.026>
- [3] D. Shin, Y. Han, *J. Powder Mater.* **32** (6), 501-508 (2025). DOI: <https://doi.org/10.4150/jpm.2025.00416>
- [4] J.Y. Park, Y.B. Weon, M.J. Jung, B.J. Choi, *Arch. Metall. Mater.* **67**, 1503-1506 (2022). DOI: <https://doi.org/10.24425/amm.2022.141082>
- [5] S.E. Potts, W.M.M. Kessels, *Coord. Chem. Rev.* **257**, 3254-3270 (2013). DOI: <https://doi.org/10.1016/j.ccr.2013.06.015>
- [6] P.O. Oviroh, R. Akbarzadeh, D. Pan, R.A.M. Coetzee, T.-C. Jen, *Sci. Technol. Adv. Mater.* **20**, 465-496 (2019). DOI: <https://doi.org/10.1080/14686996.2019.1599694>
- [7] S. Lee, T.J. Park, S.K. Kim, *J. Powder Mater.* **29**, 56-62 (2022). DOI: <https://doi.org/10.4150/kpmi.2022.29.1.56>
- [8] H.Y. Lee, J.H. Han, B.J. Choi, *J. Vac. Sci. Technol. A* **42**, 022405 (2024). DOI: <https://doi.org/10.1116/6.0003319>
- [9] M.G. Cho, S. Jeon, H.W. Kim, J.H. Park, T. Eom, B.J. Choi, *J. Mater. Chem. C* **13**, 17750-17758 (2025). DOI: <https://doi.org/10.1039/d5tc02138c>
- [10] K.E.K. Holden, S.M. Witsell, P.C. Lemaire, J.F. Conley, Jr., *J. Vac. Sci. Technol. A* **40**, 040401 (2022). DOI: <https://doi.org/10.1116/6.0001865>
- [11] K.H. Yoon, H. Kim, Y.-E. K. Lee, N.K. Shrestha, M.M. Sung, *RSC Adv.* **7**, 5601 (2017). DOI: <https://doi.org/10.1039/c6ra27759d>
- [12] S.K. Kim, S. Hoffmann-Eifert, R. Waser, *Electrochem. Solid-State Lett.* **14**, H146-H148 (2011). DOI: <https://doi.org/10.1149/1.3534833>
- [13] S.Y. No, D. Eom, C.S. Hwang, H.J. Kim, *J. Electrochem. Soc.* **153**, F87-F93 (2006). DOI: <https://doi.org/10.1149/1.2186179>
- [14] H. Kim, D.H. Kim, B.J. Choi, *Korean J. Mater. Res.* **28**, 5 (2018). DOI: <https://doi.org/10.3740/mrsk.2018.28.5.268>
- [15] G. Park, D. Go, S. Jo, T.H. Lee, J.W. Shin, *J. An, Adv. Electron. Mater.* **9**, 2300074 (2023). DOI: <https://doi.org/10.1002/aelm.202300074>